



Charmonia production in ALICE

Christophe Suires*, for the ALICE Collaboration

Institut de Physique Nucléaire d'Orsay, CNRS-IN2P3, Université Paris-Sud, France

Abstract

Quarkonia states are expected to provide essential information on the properties of the high-density strongly-interacting system formed in the early stages of high-energy heavy-ion collisions. ALICE is the LHC experiment dedicated to the study of nucleus-nucleus collisions and can study charmonia at forward rapidity ($2.5 < y < 4$) via the $\mu^+\mu^-$ decay channel and at mid rapidity ($|y| < 0.9$) via the e^+e^- decay channel. In both cases charmonia are measured down to zero transverse momentum. The inclusive J/ψ production as a function of transverse momentum and rapidity in pp collisions at $\sqrt{s} = 2.76$ and 7 TeV are presented. For pp collisions at $\sqrt{s} = 7$ TeV, the inclusive J/ψ production as a function of the charged particle multiplicity, the inclusive J/ψ polarization at forward rapidity and the J/ψ prompt to non-prompt fraction are discussed.

Finally, the analysis of the inclusive J/ψ production in the Pb-Pb data collected fall 2011 at a center of mass energy of $\sqrt{s_{NN}} = 2.76$ TeV is presented. Results on the nuclear modification factor are then shown as a function of centrality, transverse momentum and rapidity and compared to model predictions. First results on inclusive J/ψ elliptic flow are given.

Keywords: Hadron-induced high- and super-high-energy interactions, Relativistic heavy-ion collisions, Quark-Gluon plasma, J/ψ production and suppression mechanisms.

1. Charmonia in heavy-ion collisions

Charmonia suppression via color-screening of the heavy-quark potential was originally proposed as a probe of the QCD matter formed in relativistic heavy-ion collisions in 1986 [1]. J/ψ production was extensively studied at the Super Proton Synchrotron (SPS) and at the Relativistic Heavy Ion Collider (RHIC). Indeed, J/ψ suppression in most central heavy-ion collisions was observed over a large energy range (≈ 20 to 200 GeV/c). The LHC has opened a new energy regime for the study of quarkonium in heavy-ion collisions. In a Pb-Pb collision at $\sqrt{s_{NN}} = 2.76$ TeV, an average of one J/ψ particle is expected to be produced in every central Pb-Pb collision, together with about 100 $c\bar{c}$ pairs. Several models [2, 3, 4, 5] have included, already at RHIC energy, a J/ψ regeneration component from deconfined charm quarks in the medium which counteracts the J/ψ suppression in a QGP. At LHC, this regeneration component may become important, even dominant.

The in-medium modification of the J/ψ production can be quantified with the nuclear modification factor R_{AA} , defined as the J/ψ yield measured in nucleus-nucleus collisions divided by the yield measured in pp collisions and the number of binary nucleon-nucleon collisions occurring in the nucleus-nucleus collision. To interpret the R_{AA} ,

*Email: christophe.suires@ipno.in2p3.fr

one must keep in mind the following points. First, prompt J/ψ production in hadronic interactions consists of the sum of direct J/ψ ($\approx 65\%$) and excited $c\bar{c}$ states such as χ_c and $\psi(2S)$ ($\approx 35\%$). Since the χ_c and $\psi(2S)$ have lower dissociation temperatures than the J/ψ , a J/ψ R_{AA} measurement around 0.65 is compatible within errors with the suppression of excited states only. In addition to these prompt J/ψ one should also take into account that a non-prompt component from beauty hadron decays is present at LHC energy. The R_{AA} includes cold nuclear matter (CNM) effects, dominated by nuclear absorption and (anti-) shadowing. These CNM effects can be responsible for J/ψ suppression independently from the creation of a deconfined medium. To quantify CNM effects, proton-nucleus collisions are needed. At SPS energy, the observed J/ψ suppression would be compatible with the dissociation of excited states, once the CNM effects are taken into account. At RHIC, a J/ψ R_{AA} of ≈ 0.25 in most central Au-Au collisions was measured by the PHENIX experiment [6] with a strong centrality dependence. After estimating the correction due to the CNM effects, the suppression of direct J/ψ is at least $\approx 40\%$ or more. At the LHC, J/ψ are abundantly produced and detailed studies of its production are possible in both elementary and heavy-ion collisions, such as azimuthal asymmetry, polarization, R_{AA} dependence on rapidity and on transverse momentum, etc. Such studies may give us some answers about the balance between suppression and recombination mechanisms of J/ψ .

The asymmetry the azimuthal distribution of J/ψ in the plane perpendicular to the beam direction, the so-called elliptic flow or v_2 is indeed a very interesting experimental observable. When heavy-ions collide at finite impact parameter (non-central collisions), the geometrical overlap region and therefore the initial matter distribution is anisotropic and is converted into a momentum anisotropy of the produced particles. The possible onset of J/ψ production via recombination mechanisms should be, according to models, accompanied with a non-zero or possibly large v_2 value [7] at low p_T . Indeed, if charm quarks reach some level of thermalization in the medium, they may acquire an elliptic flow that can be further transferred to the J/ψ assuming the J/ψ is formed via recombination.

In the following section, the ALICE experiment and the data samples will be described. Then, J/ψ production results in pp collisions at $\sqrt{s} = 2.76$ TeV and 7 TeV will be presented. The J/ψ production in Pb-Pb collisions at $\sqrt{s_{NN}} = 2.76$ will be studied through the R_{AA} dependence on centrality, p_T and y . Finally, J/ψ elliptic flow measurement will be shown.

2. Experimental apparatus and data sample

ALICE is a general purpose heavy-ion experiment and is described in [8]. It consists of a central part covering the pseudo-rapidity $|\eta| < 0.9$ and a muon spectrometer covering $-4 < \eta < -2.5$. At forward (mid) rapidity, J/ψ production is measured in the dimuon (dielectron) decay channel; in both cases the p_T coverage extends down to zero. Only detectors that are relevant to the analysis will be presented.

At mid rapidity, the $J/\psi \rightarrow e^+e^-$ analysis makes use of the high precision tracking and particle identification of the Inner Tracking System (ITS) and the Time Projection Chamber (TPC). The ITS consists of six cylindrical layers of silicon detectors; at a radius 3.9 and 7.6 cm, the first two layers are equipped with silicon pixels (SPD), then two layers of silicon drifts at radius 15 and 23.9 cm and finally, two layers of silicon strips at radius 38 and 43 cm. Its main tasks are the primary and secondary vertex reconstruction; the resolution on the primary vertex ranges from 100 μm (pp collisions) to 10 μm (central Pb-Pb collisions). The SPD has triggering capabilities and can provide a signal at level 0. The large cylindrical TPC has full azimuthal coverage and extends from $z = -2.50$ m to $z = 2.50$ m¹. The TPC radial coverage ranges from $r = 85$ cm to $r = 247$ cm. This large drift detector is the main track reconstruction device at central rapidity since it can provide up to 159 space points per track. Particle identification (PID) is achieved via the measurement of the specific energy loss (dE/dx) of particles in the detector gas ($\text{Ne}/\text{CO}_2/\text{N}_2$). The excellent dE/dx resolution of $\approx 5\%$ allows to identify electrons by using inclusion cut around the Bethe-Bloch fit for electrons and exclusion cuts for protons and pions. ALICE has further capabilities to improve electron identification and triggering thanks to the Time-Of-Flight (TOF), the Transition Radiation Detector (TRD) and the Electromagnetic Calorimeter (EMCAL) detectors. However, these detectors have not been used in the analysis presented here.

At forward rapidity ($2.5 < y < 4$) the production of quarkonium states is measured in the muon spectrometer². The spectrometer consists of a ten interaction length thick absorber (-0.9 m $< z < -5.0$ m) filtering the muons in front

¹The z axis is defined here as the beam line axis in the counter clockwise direction and its origin is at the center of the ALICE detector.

²In the ALICE reference frame, the muon spectrometer covers a negative η range and consequently a negative y range. We have chosen to present our results with a positive y notation.

of five tracking stations (MCH) made of two planes of cathode pad chambers each. The third station is located inside a dipole magnet with a 3 Tm field integral. The MCH chambers are positioned between $z=-5.2$ and $z=-14.4$ m. The tracking apparatus is completed by a triggering system (MTR) made of two stations, located at $z=-16.1$ and $z=-17.1$ m, each equipped of two planes of resistive plate chambers. The MTR chambers are downstream of a 1.2 m thick iron wall, which absorbs secondary hadrons escaping from the front absorber and low momentum muons coming mainly from π and K decays. Throughout its full length, a conical absorber made of tungsten, lead and steel protects the muon spectrometer against secondary particles produced by the interaction of large- η primaries in the beam pipe. The forward VZERO detectors, two arrays of 32 scintillator tiles covering the range $2.8 \leq \eta \leq 5.1$ (VZERO-A) and $-3.7 \leq \eta \leq -1.7$ (VZERO-C), are positioned at $z=340$ and $z=-90$ cm. And finally, the zero degree calorimeters (ZDC) placed 116 m down and up-stream ALICE can detect spectator neutrons and protons.

In proton-proton collisions, the minimum bias (MB) trigger uses information of the SPD and VZERO detectors. It is defined as the logical OR of the three following conditions: (i) a signal in two readout chips in the outer layer of the SPD, (ii) a signal in VZERO-A, (iii) a signal in VZERO-C. This MB trigger requires the coincidence of the crossing of two proton bunches at the experiment interaction point (IP). ALICE MB trigger selects about 86% of the proton-proton inelastic cross section. Specific cross sections were measured during van der Meer scan in pp collisions at 7 and 2.76 TeV and allowed to determine the absolute normalization of the inclusive J/ψ cross section. The muon minimum bias trigger (μ -MB) requires, in addition to the MB conditions given above, a signal in the MTR system. The MTR can reconstruct a *trigger track*, determine its p_T and select different thresholds ($p_T \approx 0.5, 1$ and 4 GeV/c). The μ -MB trigger helps to take advantage of the full luminosity delivered by the LHC in the muon spectrometer. The MB trigger used in Pb-Pb collisions collected in 2010 requires the logical AND of the conditions (i),(ii) and (iii) given above. The centrality of the collision is determined from the amplitude of the VZERO signal fitted with a geometrical-Glauber model [9]. In 2011, the MB conditions were reduced to the AND of conditions (ii) and (iii) but additional requirements were added to select rare events. In particular, event multiplicity and dimuon triggers were added and ZDC were used for rejecting electromagnetic Pb-Pb interactions and satellite Pb-Pb collisions. Once the centrality selection cut has been applied, triggers are fully efficient with negligible contamination.

3. J/ψ production in pp collisions

The J/ψ production in pp collisions is extensively studied in ALICE and only a selection of the available results will be presented in this section. Further details on the related analysis can be found in [10].

The inclusive J/ψ production was measured in pp collisions at $\sqrt{s} = 7$ TeV in the dimuon and dielectron channels in the rapidity ranges $2.5 < y < 4$ and $|y| < 0.9$ down to $p_T = 0$. The analysis was made with an integrated luminosity $\mathcal{L}_{\text{int}} \approx 16$ (6) nb^{-1} in the dimuon (dielectron) channel. The measured cross section values are $\sigma_{J/\psi}(|y| < 0.9) = 10.7 \pm 1.0(\text{stat.}) \pm 1.6(\text{syst.})^{+1.6}_{-2.3}(\text{syst.pol.}) \mu\text{b}$ and $\sigma_{J/\psi}(2.5 < y < 4.) = 6.31 \pm 0.25(\text{stat.}) \pm 0.76(\text{syst.})^{+0.95}_{-1.96}(\text{syst.pol.}) \mu\text{b}$. At forward rapidity differential cross section $d^2\sigma/dp_T dy$ measurement from ALICE fully overlaps with LHCb and a good agreement is found. At mid rapidity, the situation is different since ATLAS and CMS cannot measure J/ψ with $p_T \lesssim 6$ GeV/c. Thus combining ALICE and CMS/ATLAS data offers a rather complete inclusive J/ψ production measurement over a large rapidity range. These comparisons are available in [11].

The same analysis was carried out with pp collisions at $\sqrt{s} = 2.76$ TeV collected in March 2011. Since the center of mass energy per nucleon-nucleon collisions is identical to the one of the Pb-Pb collisions, this analysis provides an essential reference data to measure the J/ψ nuclear modification factor. The integrated luminosity for the analysis is $\mathcal{L}_{\text{int}} \approx 20$ (1) nb^{-1} in the dimuon (dielectron) channel. The integrated cross sections are $\sigma_{J/\psi}(|y| < 0.9) = 6.71 \pm 1.24(\text{stat.}) \pm 1.22(\text{syst.})^{+1.01}_{-1.41}(\text{syst.pol.}) \mu\text{b}$ and $\sigma_{J/\psi}(2.5 < y < 4.) = 3.34 \pm 0.13(\text{stat.}) \pm 0.28(\text{syst.})^{+0.53}_{-1.07}(\text{syst.pol.}) \mu\text{b}$. Note that the uncertainties quoted here on the pp measurement are one of the main source of uncertainty of the nuclear modification factor discussed in the next section. The differential cross sections $d^2\sigma/dp_T dy$ have been extracted down to $p_T = 0$ at both rapidities. These results are compared to a theoretical model, NRQCD calculation that includes Color Singlet and Color Octet terms at NLO, which describes reasonably well the measurement at $\sqrt{s} = 2.76$ TeV and also the one at $\sqrt{s} = 7$ TeV [12].

In the previous results, one could remark that the J/ψ cross section has a large uncertainty related to the unknown polarization. ALICE has studied J/ψ polarization in pp collisions $\sqrt{s} = 7$ TeV in the dimuon channel. Measurements of the polar and azimuthal angle distributions of the decay muons allowed us to extract the J/ψ polarization for $2 < p_T < 8$ GeV/c and $2.5 < y < 4$. The parameters describing the J/ψ polarizations are consistent with zero in the

kinematic range under study [13]. This measurement is, at the present date, the only J/ψ polarization measurement at the LHC. It is crucial in the near future to extend the polarization measurement down to zero p_T and to high p_T in order to provide more stringent tests to theoretical calculations. In addition, since the pp cross section enters the nuclear modification factor calculation, the polarization, if different from zero, may have a strong impact at low transverse momentum. Such a measurement needs a large statistic and strengthens the requirement to collect a large amount of data at the same center of mass energy as the Pb-Pb collisions.

An interesting feature of the J/ψ production in pp collisions at $\sqrt{s} = 7$ TeV arises from its dependence on the charged particle multiplicity. The $dN_{\text{ch}}/d\eta$ is calculated from the number of tracks reconstructed in $|\eta| < 1$ using pairs of hits (tracklets) in the SPD. These measurements were performed at both rapidities in the dimuon and dielectron channels. Expressed in terms of the relative J/ψ yield $\frac{dN_{J/\psi}/d\eta}{\langle dN_{J/\psi}/d\eta \rangle}$ as a function of the relative charged multiplicity $\frac{dN_{\text{ch}}/d\eta}{\langle dN_{\text{ch}}/d\eta \rangle}$, a linear increase is clearly seen at both rapidities. For $dN_{\text{ch}}/d\eta / \langle dN_{\text{ch}}/d\eta \rangle = 4$ ($\approx 24/6$), the relative J/ψ yield is enhanced by a factor of about 5 at forward rapidity and about 8 at mid rapidity. This trend is not reproduced by PYTHIA 6.4.25 in the Perugia 2011 tune which exhibits an opposite tendency, i.e. a decrease of the J/ψ multiplicity with respect to the event multiplicity [14]. One could infer that the J/ψ production is strongly connected with the underlying hadronic activity. Whether this hadronic activity comes from multiple parton interactions remains an open question. Further investigations are needed to better understand this measurement that challenges our understanding of the J/ψ production in pp collisions. In particular, the event multiplicity dependence should be completed by the p_T dependence and extended to the open charm cross section (e.g. D mesons).

All the results presented up to now refer to inclusive J/ψ production which sums three distinct contributions: the prompt J/ψ produced directly in the pp collisions, the prompt J/ψ produced indirectly via the decay of heavier charmonia states and the non-prompt J/ψ produced in the decay of beauty hadrons. At central rapidity ($|y| < 0.9$), the measurement of the non-prompt J/ψ was achieved in pp collisions at $\sqrt{s} = 7$ TeV for $1.3 < p_T < 10$ GeV/c. This measurement is only accessible in ALICE since the other experiments cannot detect J/ψ at mid rapidity below a p_T of 6.5 GeV/c where most of the cross section lies. The integrated luminosity for the analysis is $\mathcal{L}_{\text{int}} = 5.6 \text{ nb}^{-1}$. This measurement relies on the discrimination of J/ψ produced detached from the primary vertex of the pp collisions thanks to the good spatial resolution of the ITS. By fitting simultaneously the invariant mass spectra and the pseudo-proper decay length of the reconstructed J/ψ , one can measure the relative abundances of prompt and non-prompt J/ψ , and the background. The fraction of J/ψ from beauty hadrons (f_B) in the measured kinematic range is about 15% with a strong p_T dependence. Then, f_B is combined with the inclusive J/ψ cross section measured in [11] to extract the prompt J/ψ cross section $\sigma_{J/\psi}^{\text{prompt}}(|y| < 0.9, p_T > 1.3 \text{ GeV}/c) = 7.2 \pm 0.7(\text{stat.}) \pm 1.0(\text{syst.})_{-1.2}^{+1.3}(\text{syst.pol.}) \mu\text{b}$. Comparisons with models lead to a good description of the prompt J/ψ dependence with p_T and of the total beauty cross section [15].

4. Nuclear modification factor in Pb-Pb collisions at $\sqrt{s_{\text{NN}}} = 2.76$ TeV

Inclusive J/ψ production was studied in Pb-Pb collisions at 2.76 TeV at mid and forward rapidity in the dielectron and dimuon decay channels using respectively an integrated luminosity $\mathcal{L}_{\text{int}} \approx 2.1$ and $\mathcal{L}_{\text{int}} \approx 70 \mu\text{b}^{-1}$. A crucial feature of the ALICE detector is to measure, in both channels, the J/ψ production down to $p_T = 0$ GeV/c. The large data sample analyzed in the dimuon channel allowed us to perform differential analysis of the nuclear modification factor (R_{AA}) as function of centrality, p_T , and y . In the dielectron channel, only the centrality dependence in 3 centrality classes (0–10%, 10–40% and 40–80%) could be achieved. One should note that the acceptance times efficiency factor in the dielectron (dimuon) channel is quite high $\approx 8\%$ (14%) and weakly depends on the collision centrality with a maximum relative loss of 12% (8%) from peripheral to most central collisions. Details on both analysis are given in [16]. On the left side of Fig. 1, the inclusive J/ψ R_{AA} is shown as a function of the number of nucleons participating in the collision [9] at mid and forward rapidity. At forward rapidity, a clear suppression is seen for $N_{\text{part}} > 70$ with almost no centrality dependence. These results show a good agreement with the ones published in [17] based on $\mathcal{L}_{\text{int}} \approx 2.9 \mu\text{b}^{-1}$ collected in 2010. At mid rapidity, a similar pattern could be possible but the coarser centrality classes and larger uncertainties prevent to draw any firm conclusion. The centrality integrated J/ψ R_{AA} at forward and mid rapidity are $R_{\text{AA}}^{0\%-90\%} = 0.497 \pm 0.006(\text{stat.}) \pm 0.078(\text{syst.})$ and $R_{\text{AA}}^{0\%-80\%} = 0.66 \pm 0.10(\text{stat.}) \pm 0.24(\text{syst.})$. In both cases, the systematic uncertainty is dominated by the pp reference. On the right side of Fig. 1, the centrality dependence of J/ψ R_{AA} at high- p_T is compared between ALICE and CMS [18]. A larger suppression, $R_{\text{AA}} \approx 0.25–0.30$, is measured

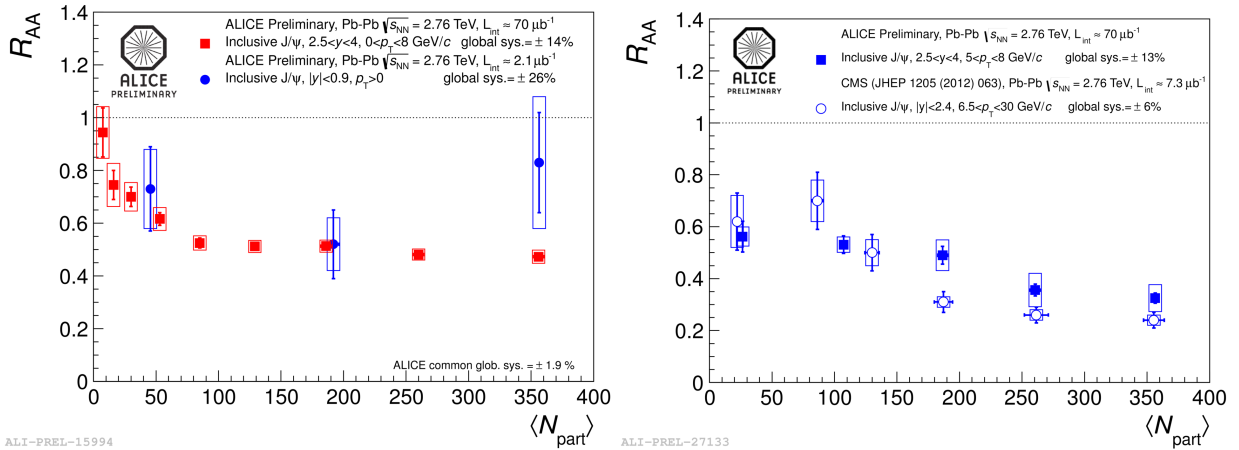


Figure 1: (Color online) Inclusive J/ψ R_{AA} measured in Pb-Pb collisions at $\sqrt{s_{NN}} = 2.76$ TeV at forward and mid rapidity in ALICE is shown on the left side. On the right side the J/ψ R_{AA} at high- p_T from ALICE at forward y is compared to one measured by CMS at central y .

in the most central collisions with a clear centrality dependence. One could see here an indication that the J/ψ R_{AA} is p_T dependent at forward rapidity and possibly at mid rapidity; selecting high- p_T J/ψ drives down the R_{AA} .

The p_T dependence of the J/ψ R_{AA} is confirmed and can be better observed in Fig. 2 (left side). The inclusive J/ψ R_{AA} is shown as a function of p_T for the 0%–90% most central Pb-Pb collisions and exhibits a decrease from 0.6 to 0.35 approximately. At high- p_T a rather direct comparison with CMS results [18] is possible; the only difference is that the CMS measurement covers a more central rapidity range ($1.6 < |y| < 2.4$). A reasonable agreement between the two measurements is found for high- p_T J/ψ R_{AA} . For p_T smaller than 4 GeV/c, the difference with PHENIX measurement [19] is striking. The PHENIX result concerns the 0%–20% most central Au-Au collisions whereas the ALICE result is for a much wider centrality range (0%–90%). However, the bulk of the J/ψ production ($\approx 60\%$) occurring in 0%–20% most central collisions, the comparison remains meaningful. In addition, work is ongoing to extract the R_{AA} versus p_T in smaller centrality classes.

The J/ψ R_{AA} dependence on rapidity has been measured over a wide range thanks to the combination of our measurement in the central barrel and in the muon spectrometer, and is displayed on the right side of Fig. 2. At forward rapidity, the J/ψ R_{AA} decreases by $\approx 40\%$ from $y = 2.5$ to $y = 4$. The measurement at mid rapidity, because of its large uncertainties, does not allow to draw a clear conclusion but hints towards a rather flat behavior between $y = 2.5$ and $y = 0$. On the same figure, an estimate of the J/ψ R_{AA} due only to shadowing effects is given for two models. Indeed at LHC energies, modification of the gluon distribution function is dominated by shadowing effects [20]. The first model is a Next to Leading Order calculation within the Color Evaporation Model [21] with the EPS09 nuclear PDF (nPDF). The second model is a Leading Order calculation within the CS Model [22] with the nDSg nPDF. In the first model, the upper and lower limits correspond to the uncertainty of the EPS09 nPDF, and in the second model the band covers the uncertainty in the factorization scale of the for nDSg PDF. One could not exclude that shadowing effects are responsible for a large part of the J/ψ suppression observed in R_{AA} from $y = 0$ to $y \approx 3$, this would imply that the expected color screening J/ψ suppression observed at lower energy (RHIC) or higher p_T (CMS) is either small or compensated by recombination mechanisms. In the rapidity range from 3 to 4, our results show that the suppression goes beyond the shadowing-only prediction given by models with our current knowledge of nPDF.

The influence of the contribution of beauty hadron feed-down to the inclusive J/ψ yield in our y and p_T range was estimated. Non-prompt J/ψ are indeed different since their suppression or production is insensitive to color screening or recombination phenomena that are expected to occur in the hot and dense medium created in the Pb-Pb collisions. The beauty hadron decay mostly occurs outside the fireball, and a measurement of the non-prompt J/ψ R_{AA} is connected to the beauty quark in-medium energy loss. At forward rapidity, the non-prompt J/ψ was measured by the LHCb collaboration to be about 10% in pp collisions at $\sqrt{s} = 7$ TeV [23] in our p_T range. Assuming the scaling of beauty production with the number of binary nucleon-nucleon collisions and neglecting the shadowing effects, the

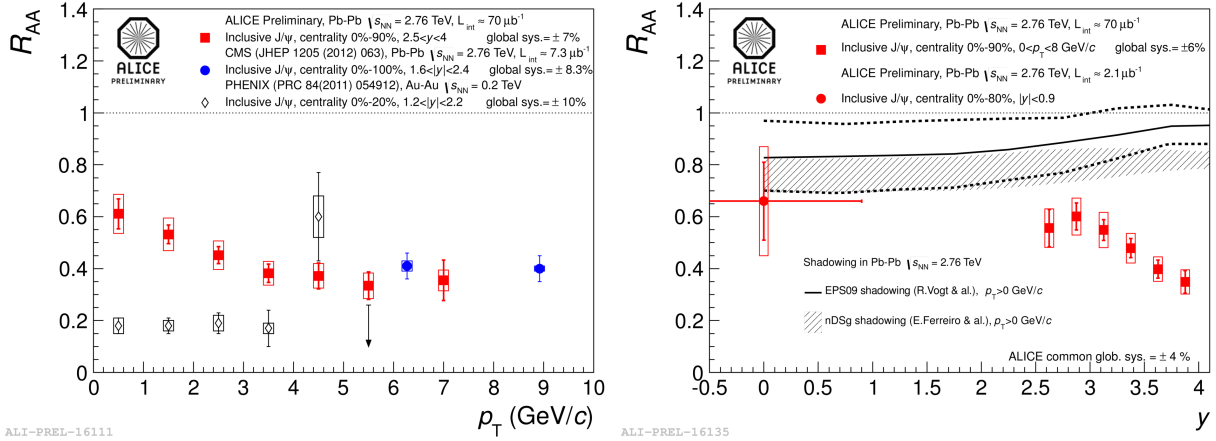


Figure 2: (Color online) ALICE p_T dependence of the inclusive J/ψ R_{AA} measured in Pb-Pb collisions at $\sqrt{s_{NN}} = 2.76$ TeV is compared to PHENIX and CMS measurements on the left side. On the right side, the rapidity dependence of the J/ψ R_{AA} measured by ALICE is compared with model predictions [21, 22] that implement only shadowing effects.

prompt J/ψ R_{AA} would be, and this is an upper limit, 11% smaller than our inclusive measurement. To estimate the influence of non-prompt J/ψ as a function of p_T and y on our inclusive R_{AA} measurement, we have extrapolated the LHCb measurement at $\sqrt{s} = 7$ TeV down $\sqrt{s} = 2.76$ TeV using an center of mass energy dependence extracted from CDF and CMS data. Assuming a range of energy loss for the beauty quarks from $R_{AA}(b) = 0.2$ to $R_{AA}(b) = 1$, we have found that the J/ψ from beauty hadrons have a negligible influence on our measurement.

In Fig. 3, our J/ψ R_{AA} measurement is compared with theoretical models that all include a J/ψ regeneration component from deconfined charm quarks in the medium. The Statistical Hadronization Model [2, 24] assumes deconfinement and a thermal equilibration of the bulk of the $c\bar{c}$ pairs. Then, charmonium production occurs only at phase boundary by statistical hadronization of charm quarks. The prediction is given for two values of $d\sigma_{c\bar{c}}/dy$ since no measurements are available at this rapidity for Pb-Pb collisions. The two transport model results [25, 26] presented in the same figure differ mostly in the rate equation controlling the J/ψ dissociation and regeneration. Both are shown as a band that connects the results obtained with (lower limit) and without (higher limit) shadowing and can be interpreted as the uncertainty of the prediction. The model from Zhao & al. implements a simple shadowing estimate leading to a 30% suppression in most central Pb-Pb collisions. The charm cross-section $d\sigma_{c\bar{c}}/dy$ at $y = 3.25$ is ≈ 0.5 mb and the J/ψ from beauty hadrons is estimated at 10% and no quenching is assumed. The model from Liu & al. takes the shadowing from EKS98 and uses a smaller charm cross-section $d\sigma_{c\bar{c}}/dy \approx 0.38$ mb. The J/ψ from beauty hadrons is estimated at 10% and b quenching is fixed at $R_{AA}(b) = 0.4$ for all the p_T range. In both transport models, the amount of regenerated J/ψ in the most central collisions contributes to about 50% of the production yield, the rest being from initial production. We can see on the left side of Fig. 3 that all three models reproduce correctly the centrality dependence of the forward J/ψ R_{AA} for $N_{part} > 70$. A similar observation can be made for the mid rapidity results [16]. The p_T dependence of the forward J/ψ R_{AA} is also successfully reproduced by the transport models, as shown on Fig. 3 right side. In addition, both models predict that a large fraction of J/ψ from regeneration have a p_T below ≈ 3.5 GeV/c.

5. Elliptic flow in Pb-Pb collisions $\sqrt{s_{NN}} = 2.76$ TeV

The elliptic flow of inclusive J/ψ has been measured as a function of the transverse momentum of the J/ψ . For this measurement, the reaction plane has been determined with the VZERO-A detector. The large rapidity gap between the J/ψ acceptance and the VZEROA detector minimizes the influence of non-flow effects. On the left side of Fig. 4, an example of the v_2 signal extraction is given; one can clearly see the cosine shape of the measured J/ψ signal in the 6 $\Delta\varphi$ bins, where $\Delta\varphi$ is the difference between the azimuthal angle of the J/ψ and the angle of the reaction plane. Further analysis details can be found in [27]. Figure 4 shows, on the right side, the first measurement of J/ψ elliptic

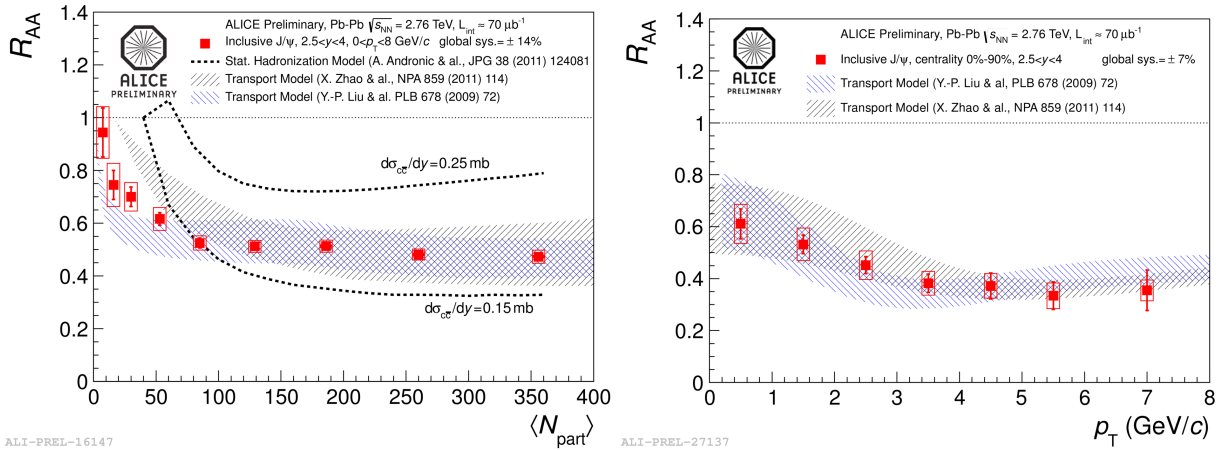


Figure 3: (Color online) Centrality and p_T dependence of the inclusive J/ψ R_{AA} measured in Pb-Pb collisions at $\sqrt{s_{NN}} = 2.76$ TeV at forward rapidity compared to the predictions by Statistical Hadronization Model [24], Transport Model I [25] and II [26], see text for details.

flow at the LHC. The J/ψ v_2 is given as a function of p_T in the 20%–60% centrality range. A non-null J/ψ v_2 seems to be present at intermediate p_T and would tend to vanish at low and high p_T . Uncertainties are still too large to draw definitive conclusions, nevertheless we have a non-zero v_2 signal for J/ψ with p_T between 2 to 4 GeV/c with 2.2σ significance. At lower energy, the J/ψ elliptic flow was measured by STAR and appear to be consistent with zero at $p_T < 10$ GeV/c in 20%–60% centrality range, whereas charged hadrons and ϕ exhibit a rather strong flow in this same kinematic domain [28]. Model prediction (private communication) for ALICE was provided by the authors of [26] and is shown on Fig. 4. The full line assumes a thermalization of the beauty quarks in the medium, for which there is no evidence so far, and should be considered as an upper limit. The dashed line, a more realistic prediction in which beauty quarks are not thermalized, shows indeed a non-zero J/ψ v_2 , which matches qualitatively our data. It is important to add that this model reproduces successfully the ALICE J/ψ R_{AA} measurement.

6. Conclusion

Quarkonia production in ALICE in pp and Pb-Pb collisions at $\sqrt{s_{NN}} = 2.76$ and 7 TeV has been presented. In pp collisions, the p_T , y and multiplicity dependence of J/ψ production, J/ψ polarization and non-prompt J/ψ have been studied. Results have shown good agreement or complementarity with other LHC results. All these measurements provide stringent constraints to model predictions. In Pb-Pb collisions, the J/ψ nuclear modification factor was studied as a function of centrality, p_T and y . The J/ψ R_{AA} dependence on the number of participant nucleons is flat and centrality integrated values are large at mid and forward rapidity ($\approx 0.7 - 0.5$). This result is clearly different from the ones seen at lower energies (e.g. RHIC and SPS). The rapidity dependence of the J/ψ R_{AA} shows that suppression at large rapidity ($2.5 < y < 4$) is beyond the one that could be expected from shadowing only predictions. The J/ψ R_{AA} is large at low p_T and then decreases with increasing p_T . The trends observed in the data as a function of centrality and p_T can be reproduced by models based on deconfinement followed by charm recombination. In these models, J/ψ from recombination mostly occur at low p_T and account for half of the produced J/ψ in the most central collisions. Finally, we have presented the J/ψ elliptic flow in semi-central Pb-Pb collisions. For the first time, a non-zero J/ψ v_2 is observed in the intermediate p_T range. We have now accumulated hints that the J/ψ production in Pb-Pb collisions at LHC energy may be governed, for an important part, by charm quarks recombination processes. In order to confirm this observation, the shadowing must be measured and constrained since it remains unknown at LHC energies and this will be addressed by a pPb run scheduled at the beginning of 2013. One should add here that the uncertainties in J/ψ R_{AA} results depend directly on the pp reference data; thus it is crucial to collect a large amount of pp collisions at the same collision energy that of Pb-Pb sample, in order to have precise measurements of J/ψ and charm differential cross section and J/ψ polarization.

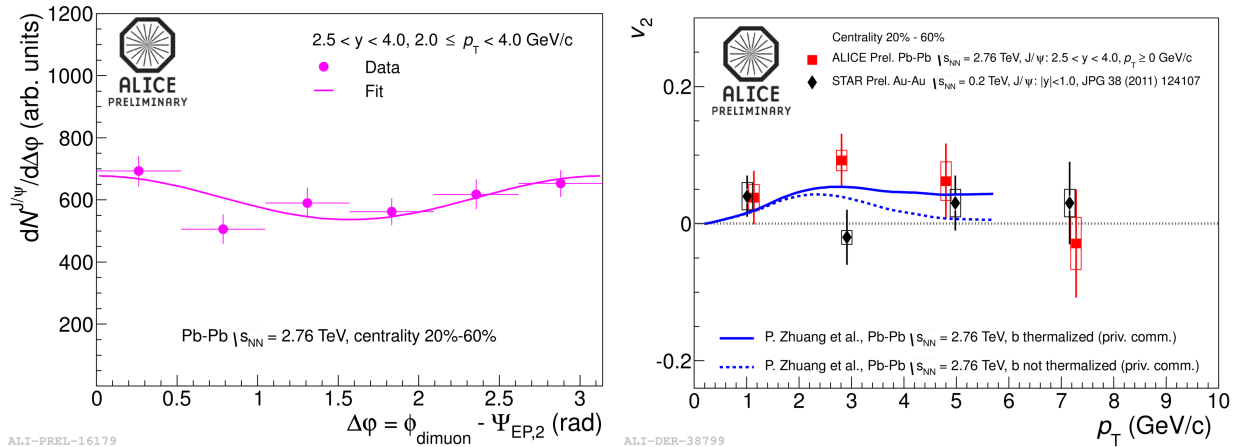


Figure 4: (Color online) Example of the J/ψ v_2 signal extraction in $\Delta\phi$ bins (left). Inclusive J/ψ v_2 measured in the 20%–60% centrality range for Pb-Pb collisions at $\sqrt{s_{NN}} = 2.76$ TeV (right side) compared to the STAR measurement and to the prediction from a parton transport model.

References

- [1] T. Matsui, H. Satz, J/ψ Suppression by Quark-Gluon Plasma Formation, Phys. Lett. B178 (1986) 416.
- [2] P. Braun-Munzinger, J. Stachel, (Non)thermal aspects of charmonium production and a new look at J/ψ suppression, Phys. Lett. B490 (2000) 196–202.
- [3] R. L. Thews, M. Schroedter, J. Rafelski, Enhanced J/ψ production in deconfined quark matter, Phys. Rev. C63 (2001) 054905.
- [4] A. Andronic, P. Braun-Munzinger, K. Redlich, J. Stachel, Evidence for charmonium generation at the phase boundary in ultra-relativistic nuclear collisions, Phys. Lett. B652 (2007) 259–261.
- [5] X. Zhao, R. Rapp, Transverse Momentum Spectra of J/ψ in Heavy-Ion Collisions, Phys. Lett. B664 (2008) 253–257.
- [6] A. Adare, et al., J/ψ production vs centrality, transverse momentum, and rapidity in Au+Au collisions at $\sqrt{s_{NN}}=200$ GeV, Phys. Rev. Lett. 98 (2007) 232301.
- [7] Y. Liu, N. Xu, P. Zhuang, J/ψ elliptic flow in relativistic heavy ion collisions, Nucl.Phys. A834 (2010) 317C–319C.
- [8] K. Aamodt, et al., The ALICE experiment at the CERN LHC, JINST 3 (2008) S08002.
- [9] K. Aamodt, et al., Centrality Dependence of the Charged-Particle Multiplicity Density at Midrapidity in Pb-Pb Collisions at $\sqrt{s_{NN}} = 2.76$ TeV, Phys. Rev. Lett. 106 (2011) 032301.
- [10] C.Geuna, Open Heavy-Flavour and J/ψ production in pp collisions measured with the ALICE experiment at LHC, these proceedings.
- [11] K. Aamodt, et al., Rapidity and transverse momentum dependence of inclusive J/ψ production in pp collisions at $\sqrt{s} = 7$ TeV, Phys.Lett. B704 (2011) 442–455. arXiv:1105.0380.
- [12] B. Abelev, et al., Inclusive J/ψ production in pp collisions at $\sqrt{s} = 2.76$ TeV, arXiv:1203.3641.
- [13] B. Abelev, et al., J/ψ polarization in pp collisions at $\sqrt{s} = 7$ TeV, Phys.Rev.Lett. 108 (2012) 082001.
- [14] B. Abelev, et al., J/ψ Production as a Function of Charged Particle Multiplicity in pp Collisions at $\sqrt{s} = 7$ TeV, Phys.Lett. B712 (2012) 165–175. arXiv:1202.2816.
- [15] B. Abelev, et al., Measurement of prompt and non-prompt J/ψ production cross sections at mid-rapidity in pp collisions at $\sqrt{s} = 7$ TeV arXiv:1205.5880.
- [16] J.Wieczula, Nuclear modification of J/ψ production in Pb-Pb collisions at $\sqrt{s_{NN}} = 2.76$ TeV, these proceedings.
- [17] B. Abelev, et al., J/ψ Suppression at Forward Rapidity in Pb-Pb Collisions at $\sqrt{s_{NN}} = 2.76$ TeV, Phys. Rev. Lett. 109 (2012) 072301.
- [18] S. Chatrchyan, et al., Suppression of non-prompt J/ψ , prompt J/ψ , and $\Upsilon(1S)$ in PbPb collisions at $\sqrt{s_{NN}} = 2.76$ TeV, JHEP 1205 (2012) 063.
- [19] A. Adare, et al., J/ψ suppression at forward rapidity in Au+Au collisions at $\sqrt{s_{NN}} = 200$ GeV, Phys.Rev. C84 (2011) 054912.
- [20] C. Lourenço, R. Vogt, H. K. Wöhri, Energy dependence of J/ψ absorption in proton-nucleus collisions, JHEP 02 (2009) 014.
- [21] R. Vogt, Cold Nuclear Matter Effects on J/ψ and Υ Production at the LHC, Phys. Rev. C81 (2010) 044903, and Priv. Comm.
- [22] E. Ferreiro, F. Fleuret, J. Lansberg, N. Matagne, A. Rakotozafindrabe, Cold Nuclear Matter Effects on extrinsic J/ψ production at $\sqrt{s_{NN}} = 2.76$ TeV at the LHC, Nucl.Phys. A855 (2011) 327–330.
- [23] R. Aaij, et al., Measurement of J/ψ production in pp collisions at $\sqrt{s}=7$ TeV, Eur.Phys.J. C71 (2011) 1645.
- [24] A. Andronic, P. Braun-Munzinger, K. Redlich, J. Stachel, The thermal model on the verge of the ultimate test: particle production in Pb-Pb collisions at the LHC, J.Phys.G G38 (2011) 124081.
- [25] X. Zhao, R. Rapp, Medium Modifications and Production of Charmonia at LHC, Nucl.Phys. A859 (2011) 114–125.
- [26] Y.-P. Liu, Z. Qu, N. Xu, P.-F. Zhuang, J/ψ Transverse Momentum Distribution in High Energy Nuclear Collisions at RHIC, Phys.Lett. B678 (2009) 72–76, and Priv. Comm.
- [27] L.Massacrier, J/ψ elliptic flow measurement in Pb-Pb collisions at forward rapidity in the ALICE experiment, these proceedings.
- [28] Z. Tang, J/ψ production and correlation in p+p and Au+Au collisions at STAR, J.Phys.G G38 (2011) 124107. arXiv:1107.0532.